Emergence of $d \pm ip$-wave superconducting state at the edge of d-wave superconductors mediated by ferromagnetic fluctuations driven by Andreev bound states

Shun Matsubara* and Hiroshi Kontani
Department of Physics, Nagoya University, Nagoya 464-8602, Japan

(Received 17 February 2020; revised manuscript received 29 April 2020; accepted 30 April 2020; published 1 June 2020)

We propose a mechanism of spin-triplet superconductivity at the edge of d-wave superconductors. Recent theoretical research on d-wave superconductors predicted that strong ferromagnetic (FM) fluctuations are induced by a high density of states due to edge Andreev bound states (ABSs). Here, we construct a linearized gap equation for the edge-induced superconductivity and perform a numerical study based on a large cluster Hubbard model with a bulk d-wave superconducting (SC) gap. We find that ABS-induced strong FM fluctuations mediate the $d \pm ip$-wave SC state, in which the time-reversal symmetry is broken. The edge-induced p-wave transition temperature T_{cp} is slightly lower than the bulk d-wave one T_{cd}, and a Majorana bound state may be created at the end point of the edge.

DOI: 10.1103/PhysRevB.101.235103

I. INTRODUCTION

In cuprate high-T_c superconductors, spin fluctuations induce various kinds of interesting phenomena. For example, d-wave superconductivity is mediated by antiferromagnetic (AFM) fluctuations [1–6]. Non-Fermi-liquid transport phenomena such as T-linear resistivity, Curie-Weiss behavior of the Hall coefficient, and the modified Kohler rule between the magnetoresistance and the Hall angle [$\Delta\rho/\rho_0 \propto (\sigma_{xy}/\sigma_{xx})^2$] are understood as the effects of strong AFM fluctuations on the Fermi liquid state [7–13]. Moreover, a recently discovered axial and uniform charge density wave (CDW) [14–17] has been theoretically understood as a spin-fluctuation-driven charge density wave due to the Aslamazov-Larkin vertex correction mechanism [18–23].

In addition, by introducing real-space structures such as surfaces and impurities, interesting nontrivial critical phenomena emerge in correlated electron systems. In cuprate superconductors, nonmagnetic impurities enhance the spin fluctuations around them [24–32]. In the two-dimensional Hubbard model with a (1,1) edge, ferromagnetic (FM) fluctuations develop along the edge [33]. These phenomena are caused by the Friedel oscillation in the local density of states (LDOS) since the high-LDOS sites near the real-space structure drive the system toward magnetic criticality.

In contrast, in superconducting (SC) states, studies of the effects of real-space structures on the electron correlation were limited until recently. Recently, several interesting impurity-induced [34,35] and surface-induced [36] critical phenomena have been analyzed theoretically. The key ingredient is the edge-induced Andreev bound state (ABS) in d-wave superconductors [37–42], which is observed in scanning tunneling microscopy experiments as a zero-bias conductance peak [43–46]. In a previous paper [36], the present authors revealed that the huge edge density of states due to the ABS triggers very strong FM fluctuations around the (1,1) edge, by carrying out the site-dependent random-phase approximation (RPA) and modified fluctuation-exchange (FLEX) approximation. In this case, strong FM fluctuations may induce exotic phenomena such as triplet superconductivity [47–51].

As is well known, the emergence of a surface- or interface-induced SC state that is not realized in the bulk has been studied very actively. Near the (1,1) edge of the $d_{x^2-y^2}$-wave superconductor, s-wave superconductivity can emerge by using the ABS, and a $d \pm is$-wave SC state is realized [52–58]. In this case, time-reversal symmetry is broken and the zero-bias conductance peak splits. In addition, the edge current flows along the edge. This emergence of time-reversal-breaking superconductivity at the domain wall is also discussed with regard to the polycrystalline $YBa_2Cu_3O_{7-x}$ (YBCO) [59–61] and twined iron-based superconductor FeSe in the nematic phase [62]. However, the site dependence of the pairing interaction has not been taken into consideration, although FM fluctuations are strongly enhanced near the edge of the Hubbard model. Recently, the emergence of fractional vortices and a supercurrent near the (1,1) edge has been proposed [63,64]. In this case, the ABS is shifted to a finite energy and the time-reversal symmetry is broken.

In this paper, we theoretically predict the emergence of triplet superconductivity near the (1,1) edge of d-wave superconductors. The origin of the triplet gap is the strong FM fluctuations triggered by the ABS due to the sign change in the d-wave SC gap. We first develop a linearized gap equation for the edge superconductivity and apply it to a two-dimensional cluster Hubbard model with a (1,1) edge in the bulk d-wave SC state. A site-dependent pairing interaction is obtained based on microscopic calculation by the RPA or GV^I-FLEX [36]. We reveal that the phase difference between the edge triplet gap and the bulk d-wave gap is $\pi/2$ in $\boldsymbol{k}$ space. That is,

*matsubara@s.phys.nagoya-u.ac.jp

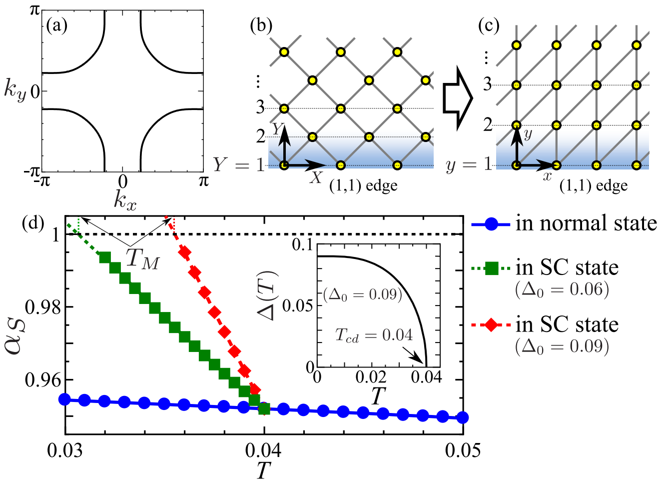

FIG. 1. (a) Fermi surface in the bulk YBCO tight-binding model at filling $n = 0.95$. (b) Square lattice with a (1,1) edge. (c) One-site unit-cell square lattice with a (1,1) edge. To simplify the calculation, we actually use the square lattice shown in (c) instead of (b). (d) T dependence of α_S in the RPA. Inset: T dependence of the bulk d-wave gap given in (4). We set the transition temperature of the d-wave superconductivity at $T_{cd} = 0.04$. At $T = T_M$, α_S reaches unity.

an exotic edge-induced $d \pm ip$-wave SC state is expected to be realized at $T = T_{cp}$, which is slightly lower than the bulk d-wave transition temperature T_{cd}. The present study may offer an interesting platform for realizing exotic SC states.

II. THEORETICAL METHOD OF THE TRIPLET GAP EQUATION

To study edge-induced triplet superconductivity, we construct a two-dimensional square lattice Hubbard model with a (1,1) edge in the bulk d-wave SC state,

$$\mathcal{H} = \sum_{i,j,\sigma} t_{i,j} c^\dagger_{i\sigma} c_{j\sigma} + U \sum_i n_{i\uparrow} n_{i\downarrow} + \sum_{i,j} (\Delta^{\uparrow\downarrow}_{i,j} c^\dagger_{i\uparrow} c^\dagger_{j\downarrow} + \text{H.c.}), \tag{1}$$

where $t_{i,j}$ is the hopping integral between site i and site j. We set the nearest, next-nearest, and third-nearest hopping integrals as $(t, t', t'') = (-1, 1/6, -1/5)$, which correspond to the YBCO tight-binding model. $c^\dagger_{i\sigma}$ and $c_{i\sigma}$ are creation and annihilation operators of an electron with spin σ, respectively. U is the on-site Coulomb interaction, and $\Delta^{\uparrow\downarrow}_{i,j} = -\Delta^{\downarrow\uparrow}_{i,j} \equiv \Delta_{i,j}$ is the bulk d-wave SC gap. Figure 1(a) shows the Fermi surface of the periodic tight-binding model at filling $n = 0.95$. In this model, AFM fluctuations develop in the bulk due to the nesting $Q \approx (\pi, \pi)$. Figure 1(b) shows the original square lattice with the (1,1) edge. If we analyze the original square lattice along the X and Y axes, there are two sites in a unit cell, and it makes the analysis complicated. For convenience, we analyze an equivalent (1,1) edge model with the one-site unit-cell structure shown in Fig. 1(c). $y = 1$ corresponds to the (1,1) edge layer. This model is periodic along the x direction, whereas the translational symmetry along the y direction is violated. Thus, we perform the following analysis in the (k_x, y, y') representation obtained by Fourier transformation only in the x direction. Here, we represent the Fourier transformation of the first term in (1) as follows:

$$H^0 = \sum_{k_x,y,y',\sigma} H^0_{y,y'}(k_x) c^\dagger_{k_x,y,\sigma} c_{k_x,y',\sigma}. \tag{2}$$

Next, we assume that $\Delta_{i,j}$ is real and nonzero only between nearest-neighbor sites and set it as $\Delta_{i,j} = \Delta/2(\delta_{x,x'+1}\delta_{y,y'+1} + \delta_{x,x'-1}\delta_{y,y'-1} - \delta_{x,x'}\delta_{y,y'+1} - \delta_{x,x'}\delta_{y,y'-1})$. By performing the Fourier transformation in the x direction, we obtain its (k_x, y, y') representation as

$$\Delta_{y,y'}(k_x, T) = \Delta(T)\left\{\frac{e^{-ik_x} - 1}{2}\delta_{y,y'+1} + \frac{e^{ik_x} - 1}{2}\delta_{y,y'-1}\right\}, \tag{3}$$

$$\Delta(T) = \Delta_0 \tanh\left(1.74\sqrt{\frac{T_{cd}}{T} - 1}\right), \tag{4}$$

where $\Delta(T)$ is the temperature-dependent d-wave gap and $\Delta_0 \equiv \Delta(T = 0)$. Note that $\Delta(\boldsymbol{k}, T) = \Delta(T)(\cos k_x - \cos k_y)$ in a bulk d-wave superconductor. T_{cd} is the transition temperature of the d-wave superconductivity. Here, we confirm the relations of the bulk d-wave gap. Due to the anticommutation relation of the fermion, the SC gap satisfies

$$\Delta_{y,y'}(k_x) \equiv \Delta^{\uparrow\downarrow}_{y,y'}(k_x) = -\Delta^{\downarrow\uparrow}_{y',y}(-k_x). \tag{5}$$

The definition of the singlet gap is

$$\Delta^{\uparrow\downarrow}_{y,y'}(k_x) = -\Delta^{\downarrow\uparrow}_{y,y'}(k_x). \tag{6}$$

Using (5) and (6), the singlet gap satisfies

$$\Delta^{\uparrow\downarrow}_{y,y'}(k_x) = \Delta^{\uparrow\downarrow}_{y',y}(-k_x). \tag{7}$$

Since we set $\Delta_{i,j}$ without loss of generality, the present real d-wave gap given by (3) satisfies

$$\Delta^{\uparrow\downarrow\,*}_{y,y'}(-k_x) = \Delta^{\uparrow\downarrow}_{y,y'}(k_x). \tag{8}$$

Hereafter, we introduce $N_y \times N_y$ matrix representations of the d-wave gap function $\hat{\Delta}(k_x)$, which is defined as $\{\hat{\Delta}(k_x)\}_{y,y'} = \Delta_{y,y'}(k_x)$.

We also define $N_y \times N_y$ Green functions in the d-wave SC state $\hat{G}$, $\hat{F}$, and $\hat{F}^\dagger$ as

$$\begin{pmatrix} \hat{G}(k_x, \varepsilon_n) & \hat{F}(k_x, \varepsilon_n) \\ \hat{F}^\dagger(k_x, \varepsilon_n) & -\hat{G}(k_x, -\varepsilon_n) \end{pmatrix} = \begin{pmatrix} \varepsilon_n \hat{1} - \hat{H}^0(k_x) & -\hat{\Delta}(k_x) \\ -\hat{\Delta}(k_x) & \varepsilon_n \hat{1} + \hat{H}^0(k_x) \end{pmatrix}^{-1}, \tag{9}$$

where $\varepsilon_n = (2n + 1)\pi i T$ is the fermion Matsubara frequency. $\hat{F}$ and $\hat{F}^\dagger$ are anomalous Green functions, which are finite only in the bulk d-wave SC state. Since the d-wave gap satisfies (6), the anomalous Green function $\hat{F}$ satisfies the relation

$$\hat{F}^{\uparrow\downarrow} = -\hat{F}^{\downarrow\uparrow} \equiv \hat{F}. \tag{10}$$

In this model, we can obtain the enhancement in the FM fluctuations at the edge by the RPA or GV^I-FLEX approximation [36].

In these analyses, we define the irreducible susceptibilities as

$$\chi^0_{y,y'}(q_x,\omega_l) = -T\sum_{k_x,n} G_{y,y'}(q_x+k_x,\omega_l+\varepsilon_n) \times G_{y',y}(k_x,\varepsilon_n), \tag{11}$$

$$\varphi^0_{y,y'}(q_x,\omega_l) = -T\sum_{k_x,n} F_{y,y'}(q_x+k_x,\omega_l+\varepsilon_n) \times F^\dagger_{y',y}(k_x,\varepsilon_n), \tag{12}$$

where $\omega_l = 2l\pi iT$ is the boson Matsubara frequency. $\hat{\varphi}^0$ is finite only in the SC state. The site-dependent spin susceptibility $\hat{\chi}^s$ is calculated using $\hat{\chi}^0$ and $\hat{\varphi}^0$ as

$$\hat{\chi}^s(q_x,\omega_l) = \hat{\Phi}(q_x,\omega_l)\{\hat{1} - U\hat{\Phi}(q_x,\omega_l)\}^{-1}, \tag{13}$$

$$\hat{\Phi}(q_x,\omega_l) = \hat{\chi}^0(q_x,\omega_l) + \hat{\varphi}^0(q_x,\omega_l). \tag{14}$$

The spin Stoner factor, α_S, is defined as the largest eigenvalue of $U\hat{\Phi}(q_x,\omega_l)$ at $\omega_l = 0$. It represents the spin fluctuation strength, and the magnetic order is realized when $\alpha_S \geqslant 1$. Figure 1(d) shows the T dependence of the Stoner factor α_S in the RPA. The inset shows the T dependence of the bulk d-wave gap given by (4). In the d-wave SC state, α_S drastically increases as T decreases due to the development of the ABS. In this case, the static spin susceptibility along the (1,1) edge layer $\chi^s_{1,1}(q_x,0)$ has a large peak at $q_x = 0$. This edge FM correlation is consistent with the bulk AFM correlation. At $T = T_M$, α_S reaches unity and edge FM order is realized.

Next, we analyze edge-induced triplet superconductivity in the presence of a bulk d-wave SC gap. Here, we represent the triplet SC gap in the (k_x, y, y') representation as $\phi^{\uparrow\downarrow}_{y,y'}(k_x)$. In this study, we do not consider the spin-orbit interaction. Then we can set the d vector as $\hat{\boldsymbol{d}}(k_x) = (0, 0, \hat{\phi}(k_x))$ without losing generality. In this case, we consider only $\phi^{\uparrow\downarrow}_{y,y'}(k_x)$ and $\phi^{\downarrow\uparrow}_{y,y'}(k_x)$.

Due to the anticommutation relation of the fermion, the SC gap satisfies

$$\phi_{y,y'}(k_x) \equiv \phi^{\uparrow\downarrow}_{y,y'}(k_x) = -\phi^{\downarrow\uparrow}_{y',y}(-k_x). \tag{15}$$

The definition of the triplet gap is

$$\phi^{\uparrow\downarrow}_{y,y'}(k_x) = \phi^{\downarrow\uparrow}_{y,y'}(k_x). \tag{16}$$

From (15) and (16), the triplet gap follows

$$\phi^{\uparrow\downarrow}_{y,y'}(k_x) = -\phi^{\uparrow\downarrow}_{y',y}(-k_x). \tag{17}$$

Here, we introduce the $N_y \times N_y$ matrix representation $\hat{\phi}(k_x)$, which is defined as $\{\hat{\phi}(k_x)\}_{y,y'} = \phi_{y,y'}(k_x)$. To determine the edge-induced SC state, we must obtain the phase difference between the bulk d-wave gap and the edge triplet gap. Although we can use the Bogoliubov–de Gennes equation, we have to perform heavy self-consistent calculations at various temperatures. To make the theoretical analysis much more efficient, we develop the linearized gap equation for the edge triplet superconductivity, by linearizing the Bogoliubov–de Gennes equation only for $\hat{\phi}$ and $\hat{\phi}^\dagger$. We set the eigenvalue of the linearized equation as λ. When $\lambda \geqslant 1$, triplet superconductivity emerges and coexists with the bulk d-wave superconductivity. In this method, by just performing diagonalization,

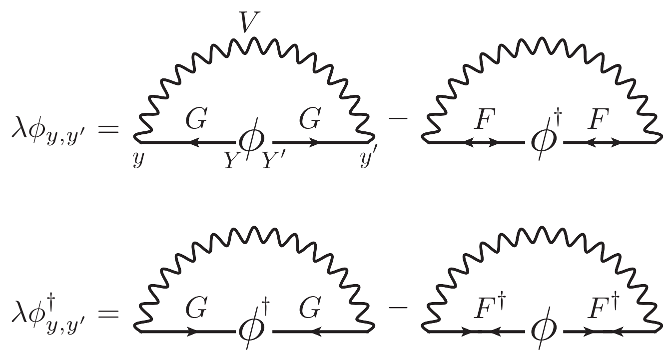

FIG. 2. Diagram of the linearized triplet SC gap equation in the presence of the bulk d-wave SC gap. The wavy lines are pairing interactions of the triplet superconductivity. The line with a single arrow represents the Green function $\hat{G}$ and the line with double arrows represents anomalous Green functions $\hat{F}$ and $\hat{F}^\dagger$.

we can address the emergence of triplet superconductivity by the temperature dependence of the eigenvalue. We show the details of the derivation of the linearized equation in Appendixes A and B. We use relations (10) and (16) in the derivation of the linearized gap equation, and it is given as

$$\begin{aligned}\lambda\phi_{y,y'}(k_x) = &-T\sum_{k'_x,Y,Y',n} V_{y,y'}(k_x-k'_x,\varepsilon_n-\varepsilon_0)\\ &\times\{G_{y,Y}(k'_x,\varepsilon_n)\phi_{Y,Y'}(k'_x)G_{y',Y'}(-k'_x,-\varepsilon_n)\\ &- F_{y,Y}(k'_x,\varepsilon_n)\phi^\dagger_{Y,Y'}(k'_x)F_{Y',y'}(k'_x,\varepsilon_n)\},\end{aligned} \tag{18a}$$

$$\begin{aligned}\lambda\phi^\dagger_{y,y'}(k_x) = &-T\sum_{k'_x,Y,Y',n} V_{y,y'}(k'_x-k_x,\varepsilon_n-\varepsilon_0)\\ &\times\{G_{Y,y}(-k'_x,-\varepsilon_n)\phi^\dagger_{Y,Y'}(k'_x)G_{Y',y'}(k'_x,\varepsilon_n)\\ &- F^\dagger_{y,Y}(k'_x,\varepsilon_n)\phi_{Y,Y'}(k'_x)F^\dagger_{Y',y'}(k'_x,\varepsilon_n)\},\end{aligned} \tag{18b}$$

$$\hat{V}(q_x,\omega_l) = U^2\left(-\tfrac{1}{2}\hat{\chi}^s(q_x) - \tfrac{1}{2}\hat{\chi}^c(q_x)\right)C(\omega_l,\omega_d), \tag{19}$$

where $\hat{V}(q_x,\omega_l)$ is the site-dependent pairing interaction for triplet superconductivity. $\hat{\chi}^{s(c)}(q_x)$ is the static spin (charge) susceptibility in the d-wave SC state obtained by the RPA or GV^I-FLEX approximation. Here, $\omega_l = 2l\pi iT$ is the boson Matsubara frequency. $C(\omega_l,\omega_d) = \omega_d^2/(|\omega_l|^2+\omega_d^2)$ is a cutoff function, where ω_d is the cutoff energy, and we set $\omega_d = 0.5$. We then solve the gap equation, (18), under the restriction (17). Note that the first and second terms in the gap equation have different signs due to relation (10). This fact greatly affects the phase difference between the bulk gap function and the edge one.

Figure 2 is a diagrammatic expression of the gap equation, (18). The undulating lines are pairing interactions $\hat{V}$. The diagrams with GG correspond to the conventional gap equation in the normal state. The diagrams with FF are newly added to describe the effect of the bulk d-wave SC gap on the edge superconductivity. Since $\hat{\phi}$ and $\hat{\phi}^\dagger$ are mixed in the present gap equation developed, Eq. (18), the phase of $\hat{\phi}$ is uniquely determined. From the viewpoint of the Ginzburg-Landau theory, the diagrams with GG and those with FF in Fig. 2, respectively, give rise to the fourth-order terms $|\Delta|^2|\phi|^2$ and

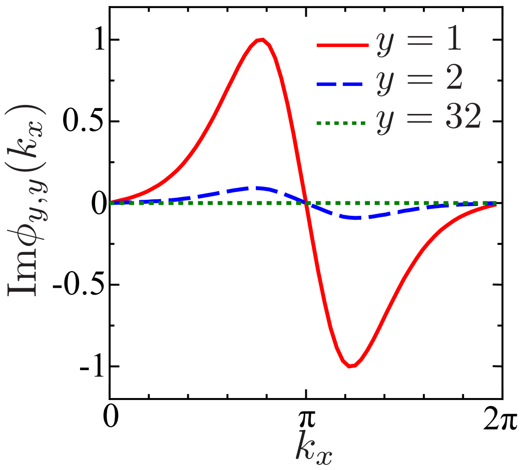

FIG. 3. k_x dependence of the obtained p_x-wave SC gap $\phi_{y,y}(k_x)$ for $\Delta_0 = 0.09$ at $T = 0.0375$. The pairing interaction is calculated by the RPA. $y = 1$ and $y = 32$ correspond to the edge and bulk, respectively. We normalize the gap as $\max_{k_x,y}|\phi_{y,y}(k_x)| = 1$.

$\mathrm{Re}\{\Delta^2\phi^{*2}\}$ in the free energy. The latter Ginzburg-Landau term determines the phase difference between $\hat{\Delta}$ and $\hat{\phi}$.

III. NUMERICAL RESULT OF THE TRIPLET GAP EQUATION

In this section, we analyze the linearized triplet gap equation, (18). The k_x mesh is $N_x = 64$, the site number along the y direction is $N_y = 64$, and the number of Matsubara frequencies is 1024. The transition temperature of the bulk d-wave superconductivity is $T_{cd} = 0.04$. The Coulomb interaction is $U = 2.25$ in the RPA and $U = 2.65$ in the GV^I-FLEX. Here, the unit of energy is $|t|$, which corresponds to ~0.4 eV in cuprate superconductors. In addition, we define $\Delta_{\max}$ as the maximum value of the d-wave gap on the Fermi surface. In the present model, $\Delta_{\max} = 1.76\Delta_0$ for $n = 0.95$. Experimentally, $4 < 2\Delta_{\max}/T_{cd} < 10$ in YBCO [65,66]. Therefore, in the RPA, we set $\Delta_0 = 0.06$ or 0.09, which corresponds to $\Delta_{\max} = 5.28$ or 7.92 for $T_{cd} = 0.04$.

A. $d \pm ip$-wave SC state

First, we analyze the linearized triplet gap equation for the pairing interaction calculated by the RPA. Figure 3 shows k_x dependence of the obtained triplet gap in the same layer y. This is the p_x-wave gap with a node at $k_x = 0$. It can emerge at the edge because there are finite LDOS values and large triplet pairing interactions due to the ABS.

Next, we discuss the phase difference between the d- and the p-wave gap. The triplet SC gap in real space $\phi_{x,y,y'}$ is represented by the Fourier transformation in the x direction of $\phi_{y,y'}(k_x)$. By using (17), we obtain

$$\phi_{x,y,y'} = -\left\{\sum_{k_x} \phi^\dagger_{y,y'}(k_x)e^{ik_x x}\right\}^*. \tag{20}$$

The relation holds for the general triplet SC gap. On the other hand, the obtained p-wave gap satisfies

$$\phi_{y,y'}(k_x) = -\phi^\dagger_{y,y'}(k_x) \tag{21}$$

in the present numerical study. Therefore, the obtained p-wave gap is a real function in real space $\phi_{x,y,y'} = \phi^*_{x,y,y'}$. In this case, the phase difference is $\pm\pi/2$ in $\boldsymbol{k}$ space, and this is the $d \pm ip$-wave SC state. We find that the edge $d \pm ip$-wave SC state is stabilized by the coexistence of bulk d-wave superconductivity and edge-induced triplet superconductivity.

The reason for this phase difference $\pm\pi/2$ is understood by evaluating the contribution from the second term in (18). Since the triplet pairing interaction $V_{y,y'}(k_x - k'_x, \varepsilon_n - \varepsilon_0)$ has a large value only at the edge ($y = 1$) and $\Delta_{i,j}$ is a real function, we can approximately evaluate the contribution to $\phi_{1,1}(k_x)$ from the second term in (18a) by setting $Y = Y' = 1$:

$$\text{second term in (18a)} \approx -T\sum_{k'_x,n} |V_{1,1}(k_x - k'_x, \varepsilon_n - \varepsilon_0)||F_{1,1}(k'_x, \varepsilon_n)|^2\phi^*_{1,1}(k'_x). \tag{22}$$

Here, $V_{y,y'}(k_x - k'_x, \varepsilon_n - \varepsilon_0)$ has a large peak at $k_x = k'_x$. Therefore, the triplet superconductivity is stabilized when $\phi^*_{1,1}(k_x) = \phi^\dagger_{1,1}(k_x) = -\phi_{1,1}(k_x)$, and it is actually confirmed by numerical calculations.

In the $d \pm ip$-wave SC state, the time-reversal (TR) symmetry is broken. To verify this, we apply the time-reversal operator $\Theta = -i\sigma^y K$ to the present gap functions:

$$\Delta^{\uparrow\downarrow}_{y,y'}(k_x) + \phi^{\uparrow\downarrow}_{y,y'}(k_x) \underset{\mathrm{TR}}{\longrightarrow} -\Delta^{\downarrow\uparrow\,*}_{y,y'}(-k_x) - \phi^{\downarrow\uparrow\,*}_{y,y'}(-k_x). \tag{23}$$

By using conditions (6), (8), (16), and (22), we confirm that the $d + ip$–wave gap changes to a $d - ip$–wave gap. In Appendix C, we calculate the LDOS in the $d \pm ip$-wave SC state. The LDOS for up-spin electrons and that for down-spin electrons are separated since the time-reversal symmetry is broken in the $d \pm ip$-wave SC state.

B. Temperature dependence of λ

Next, we examine the T dependence of the eigenvalue of the edge p-wave superconductivity. λ and $\lambda^{(n)}$ denote the eigenvalue in the d-wave SC state and normal state, respectively. Figure 4 shows the T dependence of the eigenvalue based on the RPA. $\lambda^{(n)}$ hardly increases and does not reach unity. On the other hand, λ increases drastically as T decreases and exceeds unity below $T_{cp} \lesssim T_{cd}$. At these temperatures, the $d \pm ip$-wave SC state is realized. Note that the edge FM order is realized at $T_M \lesssim T_{cp}$. For $\Delta_0 = 0.09$ ($2\Delta_{\max}/T_{cd} = 7.92$), the increase in λ is more drastic than that for $\Delta_0 = 0.06$ ($2\Delta_{\max}/T_{cd} = 5.28$) due to the stronger development of the FM fluctuations as shown in Fig. 1(d).

To examine the effect of FM fluctuations on the increase in λ, we analyze two types of gap equations, (i) and (ii), from which the effect of the d-wave gap is partially subtracted. In (i), we use the pairing interaction in the normal state $\hat{V}_{\mathrm{normal}}$ instead of $\hat{V}$ in the d-wave SC state and λ' denotes the eigenvalue. In (ii), we replace the Green functions $\hat{G}$, $\hat{F}$, and $\hat{F}^\dagger$ with those in the normal state, $\hat{G}^0$ and $\hat{F} = \hat{F}^\dagger = 0$.

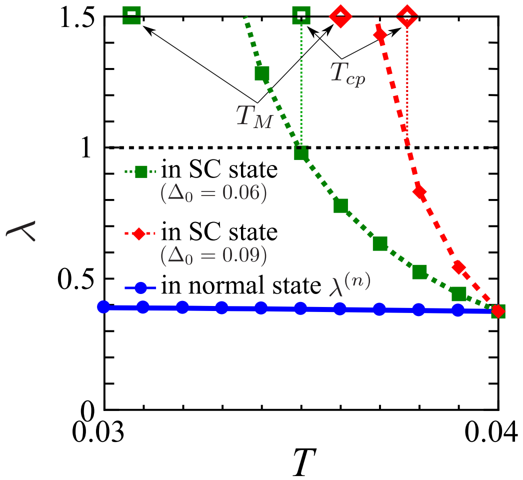

FIG. 4. T dependence of λ for the pairing interaction by the RPA. The red and green lines represent λ for $\Delta_0 = 0.06$ and 0.09, respectively. The blue line shows $\lambda^{(n)}$ in the normal state ($\Delta_0 = 0$). Below T_{cp}, p-wave superconductivity emerges. At $T = T_M$, α_S reaches unity in the RPA.

λ'' denotes the eigenvalue. Figure 5 shows the T dependence of λ' and λ''. We see that λ' is strongly suppressed, and it does not reach unity. On the other hand, λ'' is almost equal to λ and exceeds unity at $T \lesssim T_{cp}$. Therefore, the drastic increase in λ under T_{cd} is mainly due to the ABS-driven FM fluctuations.

C. Result of the GV^I-FLEX approximation

In this study, we analyze the linearized triplet gap equation for the pairing interaction calculated by the GV^I-FLEX approximation in the (1,1) edge cluster model [36]. In the conventional FLEX, the negative feedback effect on spin susceptibility near an impurity is overestimated since the vertex corrections for the spin susceptibility are not considered [32]. In the modified FLEX, cancellation between negative feedback and vertex corrections is assumed, and then reliable results are obtained for the single-impurity problem [32].

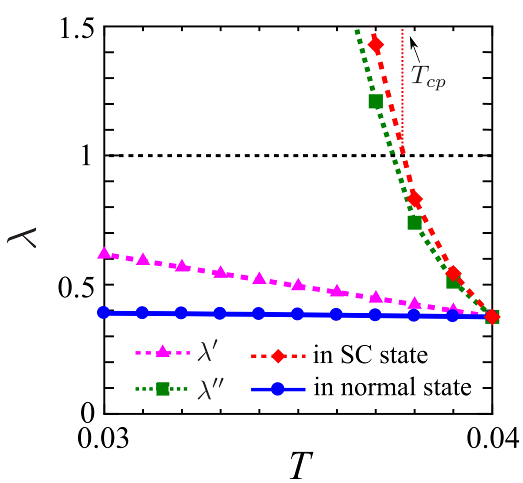

FIG. 5. T dependence of λ' and λ''. We set $\Delta_0 = 0.09$ The dotted red line and solid blue line represent λ and $\lambda^{(n)}$ in the d-wave SC state and normal state, respectively.

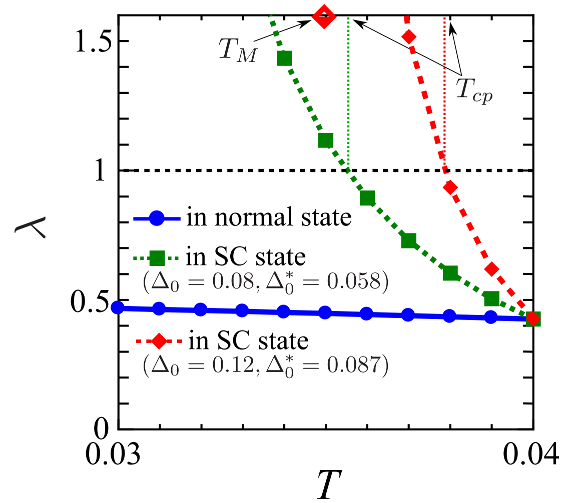

FIG. 6. T dependence of λ for the pairing interaction by GV^I-FLEX. $\Delta_0{}^*$ is the renormalized gap by the self-energy. We obtain $\Delta_0{}^* = 0.058$ for $\Delta_0 = 0.08$ and $\Delta_0{}^* = 0.087$ for $\Delta_0 = 0.12$.

$\Delta_0{}^*$ is the renormalized gap by the normal self-energy. We obtain $\Delta_0{}^* \approx 0.087$ and $2\Delta_{\max}{}^*/T_{cd} \approx 7.69$ for $\Delta_0 = 0.12$ and $\Delta_0{}^* \approx 0.058$ and $2\Delta_{\max}{}^*/T_{cd} \approx 5.11$ for $\Delta_0 = 0.08$. To simplify the analysis, the normal self-energy is not included in the Green functions in the gap equation.

Figure 6 shows the T dependence of λ based on the GV^I-FLEX. λ increases as T decreases also in the GV^I-FLEX. In the case of $\Delta_0 = 0.08$, λ exceeds unity at $T \approx 0.02$. For $\Delta_0 = 0.12$, the increase in λ is sharper than that for $\Delta_0 = 0.08$ because of the stronger development of the FM fluctuations. The increase in λ becomes milder than that by the RPA due to the negative feedback effect of self-energy. However, we obtain the emergence of a $d \pm ip$-wave superconductivity even if the self-energy is considered. Note that the T dependence of λ based on the RPA and GV^I-FLEX is comparable when $(2\Delta_{\max}/T_{cd})_{\mathrm{RPA}} \approx (2\Delta_{\max}{}^*/T_{cd})_{\mathrm{FLEX}}$.

D. Effect of finite d-wave coherence length on edge-induced triplet superconductivity

In this section, we discuss the emergence of p-wave superconductivity when the d-wave gap is suppressed for the finite range $1 \leqslant y \leqslant \xi_d$, where ξ_d is the coherence length of the d-wave superconductivity. We set the y dependence of the d-wave gap as follows:

$$\Delta_{y,y'}(k_x, T)\left(1 - \exp\left(\frac{y + y' - 2}{2\xi_d}\right)\right). \tag{24}$$

If the SC FLEX approximation [4] is applied to the edge cluster model, the obtained d-wave gap is expected to be suppressed for $y \lesssim \xi_d$. Instead, we set ξ_d as a parameter to simplify the analysis. From the experimental results [67–70], we can estimate ξ_d to be three sites for $T \ll T_{cd}$. For $T \lesssim T_{cd}$, $\xi_d \gg 3$ because of the relation $\xi_d \propto (1 - T/T_{cd})^{-1/2}$ in the Ginzburg-Landau theory. Thus, we set $\xi_d = 3$ and 10 in the present analysis.

Figure 7(a) shows the site dependence of the d-wave gap expressed by (24). Figure 7(b) shows the obtained LDOS. At

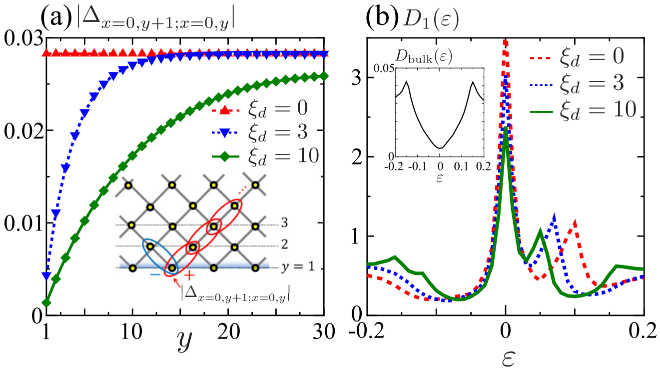

FIG. 7. (a) Site dependence of the d-wave gap suppressed near the edge over ξ_d. Inset: Nearest-neighbor bonds corresponding to $|\Delta_{x=0,y+1;x=0,y}|$. We set $\Delta_0 = 0.08$ and calculate at $T = 0.032$. (b) ε dependence of LDOS at the (1,1) edge for the d-wave gap with finite ξ_d. Inset: LDOS in the bulk ($y = 400$).

the (1,1) edge, the LDOS has a large peak at $\varepsilon = 0$ due to the ABS. Although the height of the peak becomes lower, the peak structure due to the ABS still exists for finite ξ_d. The inset illustrates the LDOS in the bulk, and it shows a V-shaped ε dependence since the d-wave gap has line nodes. In our previous paper, we confirmed that α_S increases as T decreases for finite ξ_d.

Then we analyze the gap equation based on the RPA for finite ξ_d. Figure 8 shows the T dependence of λ. For $\Delta_0 = 0.09$, λ increases as the temperature decreases and exceeds unity even for finite ξ_d. On the other hand, the increase in λ is mild for $\Delta_0 = 0.06$ and ξ_d, and $\lambda \approx 0.68$ even at $T = 0.03$. Therefore, the strong increase in λ is realized under the conditions $2\Delta_{\max}/T_{cd} \gtrsim 6$ and $\xi_d \ll 10$. These conditions are satisfied in real cuprate superconductors.

IV. CANCELLATION OF THE EDGE SUPERCURRENT IN THE $d \pm ip$-WAVE SC STATE

In the time-reversal-breaking SC state, there is a possibility of the emergence of an edge supercurrent. In this section, we calculate the edge supercurrent in the $d \pm ip$-wave SC state. The current operator for the σ-spin electron along the

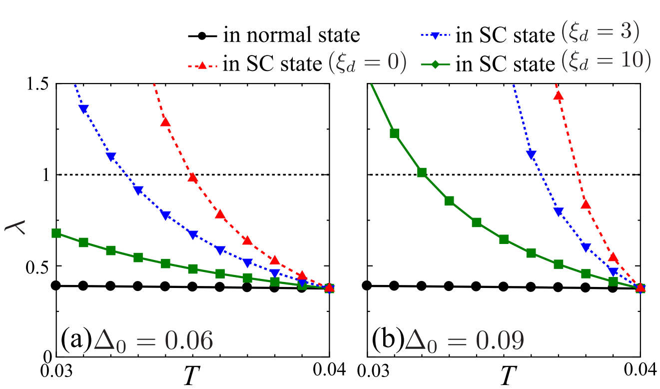

FIG. 8. T dependence of λ for (a) $\Delta_0 = 0.06$ and (b) $\Delta_0 = 0.09$ with finite ξ_d. The pairing interaction is calculated by the RPA for finite ξ_d.

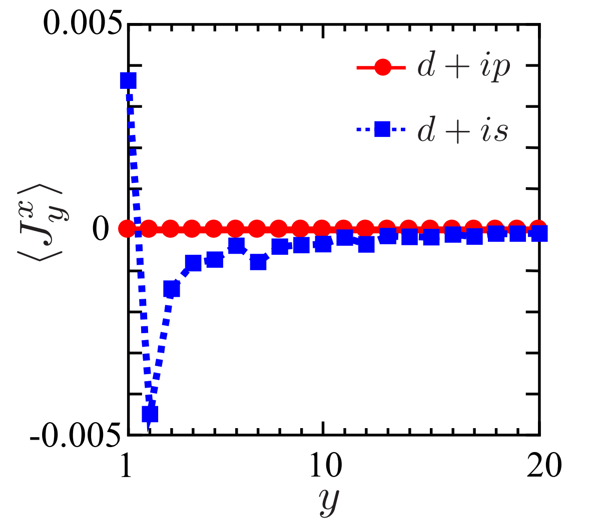

FIG. 9. y dependence of the edge supercurrent $\langle J_y^x\rangle$ in the $d + ip$– and $d + is$–wave SC state. We set $\Delta_0 = 0.09$ and $\max_{i,j}|\phi_{i,j}| = 0.09$. We set the size of the edge s-wave gap as $\Delta^s = 0.09$.

x direction is given as [71]

$$J^x_{y,y'}(k_x) = \frac{\partial}{\partial k_x} H^0_{y,y'}(k_x). \tag{25}$$

Note that $J^x_{y,y'}(k_x)$ does not include the SC gaps. The spontaneous supercurrent between layer y and layer y' is

$$\langle J^x_{y,y'}\rangle = -\frac{e}{2}\sum_{k_x}\{J^x_{y,y'}(k_x)n^{\sigma\sigma}_{y,y'}(k_x) + (y \leftrightarrow y')\}, \tag{26}$$

where $n^{\sigma\sigma}_{y,y}(k_x)$ is given as

$$\begin{aligned} n^{\sigma\alpha}_{y,y'}(k_x) &= \langle c^\dagger_{k_x,y,\sigma} c_{k_x,y',\alpha}\rangle \\ &= \sum_b U_{(y\sigma),b}(k_x) U^*_{(y'\alpha),b}(k_x) \\ &\quad \times \left\{T\sum_n \mathrm{Re}G_b(k_x,\varepsilon_n) + \frac{1}{2}\right\}. \end{aligned} \tag{27}$$

$\hat{U}$ is the unitary matrix to diagonalize the Bogoliubov–de Gennes Hamiltonian in the $d \pm ip$-wave SC state and G_b is the Green function in the band representation. We explain the Green function in the $d \pm ip$-wave SC state in Appendix A. Here, we define the edge current though layer y as

$$\langle J^x_y\rangle = \sum_{y'}\langle J^x_{y,y'}\rangle. \tag{28}$$

Then the total supercurrent is given by $\langle J^x\rangle = \sum_y \langle J^x_y\rangle$.

Figure 9 shows the obtained y dependence of the edge current in the $d + ip$– and $d + is$–wave SC state. We set the edge s-wave gap as $i\Delta^s\delta_{y,y'=1}$ and $\Delta^s = 0.09$ for simplicity. In the $d + ip$–wave SC state, the time-reversal symmetry is broken. Nonetheless, no edge current flows. On the other hand, the current flows along the edge in the $d + is$–wave SC state as pointed out in Ref. [53].

To explain why the spontaneous edge current cancels in the $d + ip$–wave SC state, we consider the Green function $G^{\uparrow\uparrow}_{y,y'}(k_x, \varepsilon_n)$, which corresponds to the transfer process of an up-spin electron from site y' to y. Here, we evaluate an example of its second-order term in proportion to $\Delta\phi^\dagger$:

$$\delta G^{\uparrow\uparrow}_{y,y'}(k_x,\varepsilon_n) = -G^0_{y,y_1}(k_x,\varepsilon_n)\Delta^{\uparrow\downarrow}_{y_1,y_2}(k_x) \times G^0_{y_3,y_2}(-k_x,-\varepsilon_n){\phi^{\uparrow\downarrow}_{y_3,y_4}}^\dagger(k_x)G^0_{y_4,y'}(k_x,\varepsilon_n), \tag{29}$$

where $G^0_{y,y'}(k_x,\varepsilon_n)$ is the Green function in the normal state. Then the inverse transfer process from (29) contributing to $G^{\uparrow\uparrow}_{y',y}(-k_x,\varepsilon_n)$ is given by

$$\begin{aligned}\delta G^{\uparrow\uparrow}_{y',y}(-k_x,\varepsilon_n) &= -G^0_{y',y_4}(-k_x,\varepsilon_n)\phi^{\uparrow\downarrow}_{y_4,y_3}(-k_x)\\ &\quad\times G^0_{y_2,y_3}(k_x,-\varepsilon_n){\Delta^{\uparrow\downarrow}_{y_2,y_1}}^\dagger(-k_x)G^0_{y_1,y}(-k_x,\varepsilon_n).\end{aligned} \tag{30}$$

Note that $\hat{G}^0$ satisfies $G^0_{y,y'}(k_x,\varepsilon_n) = G^0_{y',y}(-k_x,\varepsilon_n)$. In addition, by using (7), (8), (17), and (22), we obtain $\delta G^{\uparrow\uparrow}_{y,y'}(k_x,\varepsilon_n) = \delta G^{\uparrow\uparrow}_{y',y}(-k_x,\varepsilon_n)$. Therefore, $n^{\sigma\sigma}_{y,y'}(k_x) = n^{\sigma\sigma}_{y',y}(-k_x)$ holds and thus the current does not flow.

V. SUMMARY

In this paper, we demonstrate that the $d \pm ip$-wave SC state is realized at the (1,1) edge of d-wave superconductors due to the ABS-induced strong FM fluctuations. We study the two-dimensional cluster Hubbard model with the edge in the presence of the bulk d-wave SC gap. To analyze the edge-induced SC gap, we construct a linearized triplet SC gap equation in the presence of the bulk d-wave SC gap. The site-dependent pairing interaction is calculated using the RPA or GV^I-FLEX. The obtained phase difference between the bulk d-wave gap and the edge p-wave gap is $\pi/2$ in $\boldsymbol{k}$ space, and it is the $d \pm ip$-wave SC state in which the time-reversal symmetry is broken. Next, we examine the T dependence of the eigenvalue λ for the edge-induced SC state. Below the bulk d-wave transition temperature T_{cd}, λ for the triplet state increases drastically as T decreases, and it exceeds unity at $T = T_{cp}$. Therefore, the $d \pm ip$-wave SC state is realized at $T_{cp} \lesssim T_{cd}$. In the $d \pm ip$-wave SC state, the edge current does not flow irrespective of the time-reversal symmetry braking.

We expect that the $d \pm ip$-wave SC state is also realized when the direction of the edge is near the (1,1) edge for the following reason: The present edge p-wave SC is mediated by ABS-induced strong FM fluctuations, and the formation of the ABS is confirmed for other edges by numerical calculations [38,54,55]. For a small deviation from the (1,1) edge, FM fluctuations should develop and the emergence of the $d \pm ip$-wave SC state is expected.

The uniqueness of the linearized edge gap equation, (18), is that only the edge-induced gap is linearized, while the effect of the bulk SC gap is included unperturbatively. This equation is very useful for analyzing interesting edge-induced superconductivity in bulk superconductors. An interesting $d \pm ip$-wave state is naturally obtained owing to the interference between the bulk and the edge gap functions.

In the present study, the edge layer can be regarded as a one-dimensional p-wave superconductor since the d-wave gap vanishes in the edge layer. In Ref. [72], the emergence of a Majorana fermion at the end point of the one-dimensional p-wave superconductor is proposed. Therefore, the formation of a Majorana fermion is expected at the end point of the (1,1) edge. Thus, the present study of the edge-induced novel superconductivity induced by an ABS-driven strong correlation may offer an interesting platform for SC devices. Finally, we note that the emergence of the p-wave SC and Majorana edge state has been discussed at the interface between a bulk s-wave superconductor and magnetic material [73,74].

ACKNOWLEDGMENTS

We are grateful to Y. Tanaka, S. Onari, and Y. Yamakawa for valuable comments and discussions. This work was supported by the JSPS KAKENHI (Grants No. JP19H05825, No. JP18H01175, and No. JP19J21693).

APPENDIX A: NAMBU REPRESENTATION FOR THE COEXISTING SC STATE IN THE (k_x, y, y') REPRESENTATION

In this Appendix, we explain the Nambu representation in the (k_x, y, y') representation. We assume that the bulk d-wave gap $\Delta_{y,y'}(k_x) \equiv \Delta^{\uparrow\downarrow}_{y,y'}(k_x)$ defined in (3) and the edge triplet gap $\phi_{y,y'}(k_x) \equiv \phi^{\uparrow\downarrow}_{y,y'}(k_x)$ are both finite. First, we consider the Hamiltonian

$$H = \sum_{k,y,y',\sigma} H^0_{y,y'}(k_x)c^\dagger_{k_x,y,\sigma}c_{k_x,y,\sigma} + \frac{1}{2}\sum_{k_x,y,y',\sigma\rho}\{D^{\sigma\rho}_{y,y'}(k_x)c^\dagger_{k_x,y,\sigma}c^\dagger_{-k_x,y',\rho} + \text{H.c.}\}, \tag{A1}$$

where $D^{\sigma\rho}_{y,y'}(k_x)$ is the total gap function, which includes both the singlet d-wave gap and the triplet gap. σ and ρ represent the spin index. In this study, we ignore the spin-orbit interaction, so we can set the d vector as $\hat{\boldsymbol{d}}(k_x) = (0, 0, \hat{\phi}(k_x))$, where a hat indicates the $N_y \times N_y$ matrix of sites. Then the total gap is given by

$$\hat{D}(k_x) = i\hat{d}_0(k_x)\sigma_2 + i\hat{\boldsymbol{d}}(k_x)\cdot\boldsymbol{\sigma}\sigma_2 = \begin{pmatrix} 0 & \hat{\Delta}(k_x)+\hat{\phi}(k_x) \\ -\hat{\Delta}(k_x)+\hat{\phi}(k_x) & 0 \end{pmatrix}, \tag{A2}$$

where $\boldsymbol{\sigma} = (\sigma_1, \sigma_2, \sigma_3)$ is the Pauli matrix for spin space. Then we obtain the $2N_y \times 2N_y$ Nambu representation as

$$H = \sum_{k_x}({}^t\hat{c}^\dagger_{k_x,\uparrow}, {}^t\hat{c}_{-k_x,\downarrow})\begin{pmatrix} \hat{H}^0(k_x) & \hat{D}^{\uparrow\downarrow}(k_x) \\ \{\hat{D}^{\uparrow\downarrow}(k_x)\}^\dagger & -\hat{H}^0(-k_x) \end{pmatrix} \times \begin{pmatrix} \hat{c}_{k_x,\uparrow} \\ \hat{c}^\dagger_{-k_x,\downarrow} \end{pmatrix}, \tag{A3}$$

where $\hat{c}_{k_x,\uparrow}$ and $\hat{c}^\dagger_{-k_x,\downarrow}$ represent the N_y-component column vector of sites. The corresponding Nambu Green function is

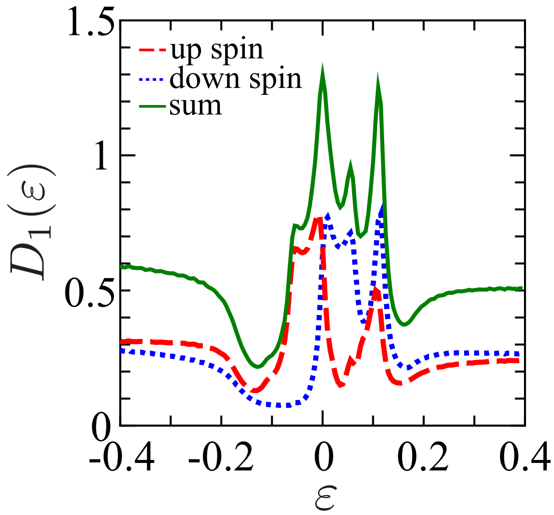

FIG. 10. ε dependence of the LDOS at the (1,1) edge in the $d + ip$–wave SC state. We set $\Delta_0 = 0.09$ and $\max_{i,j}|\phi_{i,j}| = 0.05$. The dashed red line and dotted blue line represent the LDOS for up and down spin, respectively. The solid green line shows the sum of spins.

given as

$$\begin{pmatrix} \hat{\mathcal{G}}^{\uparrow\uparrow}(k_x, \varepsilon_n) & \hat{\mathcal{F}}^{\uparrow\downarrow}(k_x, \varepsilon_n) \\ \hat{\mathcal{F}}^{\dagger\uparrow\downarrow}(k_x, \varepsilon_n) & -{}^t\hat{\mathcal{G}}^{\downarrow\downarrow}(-k_x, -\varepsilon_n) \end{pmatrix} = \begin{pmatrix} \varepsilon_n \hat{1} - \hat{H}^0(k_x) & -\hat{D}^{\uparrow\downarrow}(k_x) \\ -\{\hat{D}^{\uparrow\downarrow}(k_x)\}^\dagger & \varepsilon_n \hat{1} + {}^t\hat{H}^0(-k_x) \end{pmatrix}^{-1}. \tag{A4}$$

$\hat{\mathcal{G}}$, $\hat{\mathcal{F}}$, and $\hat{\mathcal{F}}^\dagger$ are the $N_y \times N_y$ Green functions in the coexisting SC state. The Green function in the band representation G_b in Sec. IV is obtained by using the superconducting gap equation expressed as the unitary matrix $\hat{U}$ in (A4). In this study, we do not consider the frequency dependence of the gap function. Then the total gap is represented by the anomalous Green function as

$$D^{\uparrow\downarrow}_{y,y'}(k_x, \varepsilon_n) = T \sum_{k'_x, n', \sigma} V^{\uparrow\downarrow\sigma\bar{\sigma}}_{y,y'}(k_x - k'_x, \varepsilon_n - \varepsilon'_n)\mathcal{F}^{\sigma\bar{\sigma}}_{y,y'}(k'_x, \varepsilon'_n), \tag{A5}$$

where $V^{\rm triplet}_{y,y'}(q_x, i\omega_n)$ is the pairing interaction. $\bar{\sigma}$ represents the opposite spin to σ. In the analysis in the text, we do not consider the frequency dependence of the gap function.

APPENDIX B: DERIVATION OF THE LINEARIZED TRIPLET GAP EQUATION

In this Appendix, we derive the linearized triplet gap equation in the presence of the bulk d-wave gap. First, we extract the triplet component $\phi_{y,y'}(k_x)$ from (A5) by considering the relation $\phi_{y,y'}(k_x) = \{D^{\uparrow\downarrow}_{y,y'}(k_x) + D^{\downarrow\uparrow}_{y,y'}(k_x)\}/2$. Then we obtain the equation for the triplet gap $\phi_{y,y'}(k_x)$ as

$$\phi_{y,y'}(k_x) = T \sum_{k'_x, n} V^{\rm triplet}_{y,y'}(k_x - k'_x, \varepsilon_n - \varepsilon_0)F^{\rm triplet}_{y,y'}(k'_x, \varepsilon_n), \tag{B1}$$

where $F^{\rm triplet}_{y,y'}(k_x, \varepsilon_n) \equiv \{\mathcal{F}^{\uparrow\downarrow}_{y,y'}(k_x, \varepsilon_n) + \mathcal{F}^{\downarrow\uparrow}_{y,y'}(k_x, \varepsilon_n)\}/2$ is the triplet part of the anomalous Green function in the coexisting SC state. $V^{\rm triplet}_{y,y'}(q_x, i\omega_n) \equiv V^{\uparrow\downarrow\uparrow\downarrow}_{y,y'}(q_x, i\omega_n) + V^{\uparrow\downarrow\downarrow\uparrow}_{y,y'}(q_x, i\omega_n)$ is the pairing interaction for the triplet SC, which corresponds to (20). Here, we derive the linearized triplet gap equation in the presence of a finite d-wave gap from (B1). For this purpose, we expand the full Nambu Green function in (A4) with respect to $\hat{\phi}$ and $\hat{\phi}^\dagger$, using the identity

$$\begin{aligned}(A4) &= \left\{\begin{pmatrix} \hat{G} & \hat{F} \\ \hat{F}^\dagger & -\hat{\bar{G}} \end{pmatrix}^{-1} - \begin{pmatrix} 0 & \hat{\phi} \\ \hat{\phi}^\dagger & 0 \end{pmatrix}\right\}^{-1} \\ &= \begin{pmatrix} \hat{G} & \hat{F} \\ \hat{F}^\dagger & -\hat{\bar{G}} \end{pmatrix} \\ &\quad + \begin{pmatrix} \hat{G}\hat{\phi}\hat{F}^\dagger + \hat{F}\hat{\phi}^\dagger\hat{G} & -\hat{G}\hat{\phi}\hat{\bar{G}} + \hat{F}\hat{\phi}^\dagger\hat{F} \\ \hat{F}^\dagger\hat{\phi}\hat{F}^\dagger - \hat{\bar{G}}\hat{\phi}^\dagger\hat{G} & -\hat{F}^\dagger\hat{\phi}\hat{\bar{G}} - \hat{\bar{G}}\hat{\phi}^\dagger\hat{F} \end{pmatrix} \\ &\quad + \text{ higher-order terms of } \phi \text{ and } \phi^\dagger,\end{aligned} \tag{B2}$$

where $\hat{G} \equiv \hat{G}(k_x, \varepsilon_n)$, $\hat{F} \equiv \hat{F}(k_x, \varepsilon_n)$, $\hat{F}^\dagger \equiv \hat{F}^\dagger(k_x, \varepsilon_n)$, and $\hat{\bar{G}} \equiv {}^t\hat{G}(-k_x, -\varepsilon_n)$ are the Green functions in the pure d-wave SC state introduced in (9) in the text. On the right-hand side of Eq. (B2), the first and the second terms corresponds to the zeroth-order and the first-order terms with respect to $\hat{\phi}$ or $\hat{\phi}^\dagger$, respectively. Since $\hat{F}$ satisfies the relation in (10), we obtain the relation $\hat{F}^{\rm triplet} = -\hat{G}\hat{\phi}\hat{\bar{G}} + \hat{F}\hat{\phi}^\dagger\hat{F}$. By substituting it into (B1), we obtain the linearized triplet gap equation in the presence of a bulk d-wave gap, Eq. (18a). We obtain the Eq. (18b) in the same way. The triplet gap becomes finite when the eigenvalue λ in Eqs. (18a) and (18b) reaches unity.

APPENDIX C: LDOS IN THE $d \pm ip$-WAVE SC STATE

Here, we discuss the LDOS in the $d + ip$–wave SC state. We assume that the d vector of the p-wave superconductivity is normal to the xy plane. We use the p-wave gap obtained by numerical analysis. The LDOS is given by

$$D_y(\varepsilon) = \frac{1}{\pi} \sum_{k_x, \sigma} {\rm Im}\mathcal{G}^{\sigma,\sigma}_{y,y}(k_x, \varepsilon - i\delta). \tag{C1}$$

We set $\delta = 0.01$ in the numerical calculation. Figure 10 shows the LDOS obtained at the edge. The LDOS for up-spin electrons and that for down-spin electrons are separated since the time-reversal symmetry is broken in the $d \pm ip$-wave SC state.

[1] N. E. Bickers and S. R. White, Phys. Rev. B **43**, 8044 (1991).
[2] P. Monthoux and D. J. Scalapino, Phys. Rev. Lett. **72**, 1874 (1994).
[3] S. Koikegami, S. Fujimoto, and K. Yamada, J. Phys. Soc. Jpn. **66**, 1438 (1997).
[4] T. Takimoto and T. Moriya, J. Phys. Soc. Jpn. **66**, 2459 (1997).

[5] T. Dahm, D. Manske, and L. Tewordt, Europhys. Lett. **55**, 93 (2001).
[6] D. Manske, I. Eremin, and K. H. Bennemann, Phys. Rev. B **67**, 134520 (2003).
[7] T. Moriya and K. Ueda, Adv. Phys. **49**, 555 (2000).
[8] T. Moriya and K. Ueda, Rep. Prog. Phys. **66**, 1299 (2003).
[9] P. Monthoux and D. Pines, Phys. Rev. B **47**, 6069 (1993).
[10] H. Kontani, Rep. Prog. Phys. **71**, 026501 (2008).
[11] H. Kontani, K. Kanki, and K. Ueda, Phys. Rev. B **59**, 14723 (1999).
[12] H. Kontani, J. Phys. Soc. Jpn. **70**, 2840 (2001); Phys. Rev. Lett. **89**, 237003 (2002).
[13] H. Kontani, Phys. Rev. B **64**, 054413 (2001).
[14] G. Ghiringhelli, M. L. Tacon, M. Minola, S. Blanco-Canosa, C. Mazzoli, N. B. Brookes, G. M. D. Luca, A. Frano, D. G. Hawthorn, F. He, T. Loew, M. M. Sala, D. C. Peets, M. Salluzzo, E. Schierle, R. Sutarto, G. A. Sawatzky, E. Weschke, B. Keimer, and L. Braicovich, Science **337**, 821 (2012).
[15] J. Chang, E. Blackburn, A. T. Holmes, N. B. Christensen, J. Larsen, J. Mesot, R. Liang, D. A. Bonn, W. N. Hardy, A. Watenphul, M. von Zimmermann, E. M. Forgan, and S. M. Hayden, Nat. Phys. **8**, 871 (2012).
[16] K. Fujita, M. H. Hamidian, S. D. Edkins, C. K. Kim, Y. Kohsaka, M. Azuma, M. Takano, H. Takagi, H. Eisaki, S. Uchida, A. Allais, M. J. Lawler, E. A. Kim, S. Sachdev, and J. C. Davis, Proc. Natl. Acad. Sci. USA **111**, E3026 (2014).
[17] Y. Sato, S. Kasahara, H. Murayama, Y. Kasahara, E.-G. Moon, T. Nishizaki, T. Loew, J. Porras, B. Keimer, T. Shibauchi, and Y. Matsuda, Nat. Phys. **13**, 1074 (2017).
[18] Y. Wang and A. V. Chubukov, Phys. Rev. B **90**, 035149 (2014).
[19] E. Berg, E. Fradkin, S. A. Kivelson, and J. M. Tranquada, New J. Phys. **11**, 115004 (2009).
[20] M. A. Metlitski and S. Sachdev, New J. Phys. **12**, 105007 (2010); S. Sachdev and R. La Placa, Phys. Rev. Lett. **111**, 027202 (2013).
[21] S. Onari, Y. Yamakawa, and H. Kontani, Rev. Lett. **116**, 227001 (2016).
[22] Y. Yamakawa and H. Kontani, Phys. Rev. Lett. **114**, 257001 (2015).
[23] K. Kawaguchi, Y. Yamakawa, M. Tsuchiizu, and H. Kontani, J. Phys. Soc. Jpn. **86**, 063707 (2017).
[24] P. Mendels, J. Bobroff, G. Collin, H. Alloul, M. Gabay, J. F. Marucco, N. Blanchard, and B. Grenier, Europhys. Lett. **46**, 678 (1999).
[25] K. Ishida, Y. Kitaoka, K. Yamazoe, K. Asayama, and Y. Yamada, Phys. Rev. Lett. **76**, 531 (1996).
[26] A. V. Mahajan, H. Alloul, G. Collin, and J. F. Marucco, Phys. Rev. Lett. **72**, 3100 (1994).
[27] W. A. MacFarlane, J. Bobroff, H. Alloul, P. Mendels, N. Blanchard, G. Collin, and J.-F. Marucco, Phys. Rev. Lett. **85**, 1108 (2000).
[28] A. V. Mahajan, H. Alloul, G. Collin, and J. F. Marucco, Eur. Phys. J. B **13**, 457 (2000).
[29] J. Bobroff, W. A. MacFarlane, H. Alloul, P. Mendels, N. Blanchard, G. Collin, and J.-F. Marucco, Phys. Rev. Lett. **83**, 4381 (1999).
[30] N. Bulut, Phys. Rev. B **61**, 9051 (2000).
[31] Y. Ohashi, J. Phys. Soc. Jpn. **70**, 2054 (2001).
[32] H. Kontani and M. Ohno, Phys. Rev. B **74**, 014406 (2006); J. Magn. Magn. Mater. **310**, 483 (2007).
[33] S. Matsubara, Y. Yamakawa, and H. Kontani, J. Phys. Soc. Jpn. **87**, 073705 (2018).
[34] J. W. Harter, B. M. Andersen, J. Bobroff, M. Gabay, and P. J. Hirschfeld, Phys. Rev. B **75**, 054520 (2007).
[35] B. M. Andersen, A. Melikyan, T. S. Nunner, and P. J. Hirschfeld, Phys. Rev. Lett. **96**, 097004 (2006).
[36] S. Matsubara and H. Kontani, Phys. Rev. B **101**, 075114 (2020).
[37] C. R. Hu, Phys. Rev. Lett. **72**, 1526 (1994).
[38] Y. Tanaka and S. Kashiwaya, Phys. Rev. Lett. **74**, 3451 (1995).
[39] S. Kashiwaya, Y. Tanaka, M. Koyanagi, and K. Kajimura, Phys. Rev. B **53**, 2667 (1996).
[40] M. Matsumoto and H. Shiba, J. Phys. Soc. Jpn. **64**, 1703 (1995).
[41] Y. Nagato and K. Nagai, Phys. Rev. B **51**, 16254 (1995).
[42] S. Kashiwaya and Y. Tanaka, Rep. Prog. Phys. **63**, 1641 (2000).
[43] S. Kashiwaya, Y. Tanaka, M. Koyanagi, H. Takashima, and K. Kajimura, Phys. Rev. B **51**, 1350 (1995).
[44] I. Iguchi, W. Wang, M. Yamazaki, Y. Tanaka, and S. Kashiwaya, Phys. Rev. B **62**, R6131 (2000).
[45] J. Y. T. Wei, N.-C. Yeh, D. F. Garrigus, and M. Strasik, Phys. Rev. Lett. **81**, 2542 (1998).
[46] J. Geek, X. X. Xi, and G. Linker, Z. Phys. B **73**, 329 (1988).
[47] D. Fay and J. Appel, Phys. Rev. B **22**, 3173 (1980).
[48] P. Monthoux and G. G. Lonzarich, Phys. Rev. B **59**, 14598 (1999).
[49] Z. Wang, W. Mao, and K. Bedell, Phys. Rev. Lett. **87**, 257001 (2001).
[50] R. Roussev and A. J. Millis, Phys. Rev. B **63**, 140504(R) (2001).
[51] S. Fujimoto, J. Phys. Soc. Jpn. **73**, 2061 (2004).
[52] M. Matsumoto and H. Shiba, J. Phys. Soc. Jpn. **64**, 3384 (1995).
[53] M. Matsumoto and H. Shiba, J. Phys. Soc. Jpn. **64**, 4867 (1995).
[54] M. Matsumoto and H. Shiba, J. Phys. Soc. Jpn. **65**, 2194 (1995).
[55] Y. Tanuma, Y. Tanaka, M. Ogata, and S. Kashiwaya, Phys. Rev. B **60**, 9817 (1999).
[56] S. Kashiwaya, Y. Tanaka, M. Koyanagi, H. Takashima, and K. Kajimura, J. Phys. Chem. Solids **56**, 1721 (1995).
[57] Y. Tanaka, Y. Tanuma, and S. Kashiwaya, Phys. Rev. B **64**, 054510 (2001).
[58] Y. Tanuma, Y. Tanaka, and S. Kashiwaya, Phys. Rev. B **64**, 214519 (2001).
[59] K. Kuboki and M. Sigrist, J. Phys. Soc. Jpn. **65**, 361 (1995).
[60] M. Sigrist, K. Kuboki, P. A. Lee, A. J. Millis, and T. M. Rice, Phys. Rev. B **53**, 2835 (1996).
[61] K. Kuboki and M. Sigrist, J. Phys. Soc. Jpn. **67**, 2873 (1998).
[62] T. Watashige, Y. Tsutsumi, T. Hanaguri, Y. Kohsaka, S. Kasahara, A. Furusaki, M. Sigrist, C. Meingast, T. Wolf, H. v. Löhneysen, T. Shibauchi, and Y. Matsuda, Phys. Rev. X **5**, 031022 (2015).
[63] M. Håkansson, T. Löfwander, and M. Fogelström, Nat. Phys. **11**, 755 (2015).
[64] P. Holmvall, A. B. Vorontsov, M. Fogelström, and T. Löfwander, Nat. Commun. **9**, 2190 (2018).
[65] D. S. Inosov, J. T. Park, A. Charnukha, Y. Li, A. V. Boris, B. Keimer, and V. Hinkov, Phys. Rev. B **83**, 214520 (2011).
[66] Ø. Fischer, M. Kugler, I. Maggio-Aprile, C. Berthod, and C. Renner, Rev. Mod. Phys. **79**, 353 (2007).
[67] Y. Matsuda, T. Hirai, S. Komiyama, T. Terashima, Y. Bando, K. Iijima, K. Yamamoto, and K. Hirata, Phys. Rev. B **40**, 5176 (1989).
[68] K. Semba, A. Matsuda, and T. Ishii, Phys. Rev. B **49**, 10043 (1994).

[69] K. Tomimoto, I. Terasaki, A. I. Rykov, T. Mimura, and S. Tajima, Phys. Rev. B **60**, 114 (1999).

[70] F. Izumi, H. Asano, T. Ishigaki, A. Ono, and F. P. Okamura, Jpn. J. Appl. Phys. **26**, L611 (1987).

[71] A. C. Durst and P. A. Lee, Phys. Rev. B **62**, 1270 (2000).

[72] A. Y. Kitaev, Phys. Usp. **44**, 131 (2001).

[73] S. Nakosai, Y. Tanaka, and N. Nagaosa, Phys. Rev. B **88**, 180503(R) (2013).

[74] W. Chen and A. P. Schnyder, Phys. Rev. B **92**, 214502 (2015).